MSc Computational Science
joint programme UvA/VU

MODELLING DIFFUSIVE SIGNALLING IN *ASPERGILLUS* SPP. GERMINATION INHIBITION

INTERMEDIATE PRESENTATION - APRIL

Presented by Boyan Mihaylov

April 25, 2025

Supervisor: Prof. dr. Han Wösten, Utrecht University

Examiner: Dr. Jaap Kaandorp, University of Amsterdam

OUTLINE

1 Alignment of computational methods
- Overview
- Volume-based saturation formula
- Overall model comparison

2 Single-spore experiments: revision
- Introduction
- Glucose as a reference molecule
- Diffusion and permeation constants
- Inhibitor concentrations
- Single-spore release scenarios

3 Spore cluster experiments: revision
- Introduction
- Homogeneous vs. cell-wall-bound inhibitor
- Extreme cases
- Functional relationship

4 Next steps

ALIGNMENT OF COMPUTATIONAL METHODS

Overview

- The topic of permeation and diffusion can be approached on different scales and with different formulations. The following models have been developed so far.
- Numerical models (produce simulations)
  - **Macroscopic scale** - the spore is 4 times smaller than the lattice subdivision (volume considered negligible), releases/absorbs concentration at a source site.
  - **Spore scale** - the spore is a special node on the lattice.
  - **Cell wall scale** - the spore is a voxelised sphere.
- Analytical models (produce mathematical formulas)
  - **Simple permeation** - the spore is a spherical volume that "leaks" based on the trans-barrier concentration drop.
  - **Permeation + saturation** - under high spore densities, the outside medium saturates.

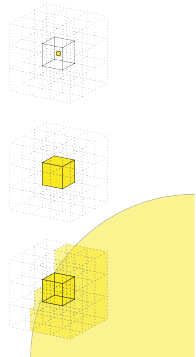

ALIGNMENT OF COMPUTATIONAL METHODS

Volume-based saturation formula

- The latest analytical model yields results closest to all other models.
- At a given spore density ρ_s, a spore has a designated volume V_{cell} around it, consisting of its own volume and the volume of the medium ($V_s + V_{\text{free}}$).
- The volume fraction $\phi = \rho_s V_s$ represents the part of the space occupied by the spore.
- It is assumed that the inhibitor diffuses fast in the medium, so its dynamics in V_{free} can be simplified.

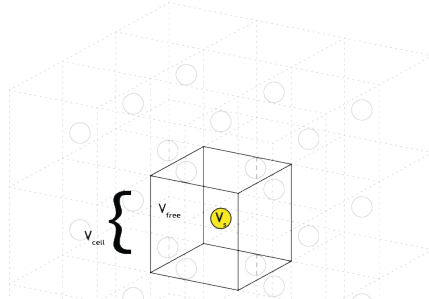

ALIGNMENT OF COMPUTATIONAL METHODS

Volume-based saturation formula

- Consider the flux through a barrier, driven by the concentration drop:

$$J(t) = P_s A \left[c_{\text{in}}(t) - c_{\text{out}}(t)\right]. \tag{1}$$

- The inside and outside concentrations change over time as

$$\dot{c}_{\text{in}} = \tau^{-1} \left(c_{\text{in}} - c_{\text{out}}\right) \tag{2}$$

$$\dot{c}_{\text{out}} = \tau^{-1} \frac{V_s}{V_{\text{free}}} \left(c_{\text{in}} - c_{\text{out}}\right). \tag{3}$$

- They reach the long-time equilibrium limit

$$c_{\text{eq}} = \rho_s \left[V_s\, c_0 + \left(\frac{1}{\rho_s} - V_s\right) c_{\text{ex}}\right] = \phi c_0 + (1-\phi) c_{\text{ex}} \tag{4}$$

-

$$\tau = \frac{V_s}{P_s A} \tag{5}$$

-

$$c_{\text{in}}(0) = c_0 \tag{6}$$

-

$$c_{\text{out}}(0) = c_{\text{ex}} \tag{7}$$

ALIGNMENT OF COMPUTATIONAL METHODS

Volume-based saturation formula

- The system of ODEs has an eigenvalue

$$\lambda_1 = -\tau^{-1}\left(1 + \frac{V_s}{V_{\text{free}}}\right) = -\tau^{-1}\left(\frac{1}{1-\phi}\right). \quad (8)$$

- This means that the characteristic time for the concentration release (modulated by density) is

$$\tau_{\text{eff}} = -\frac{1}{\lambda_1} = \tau(1-\phi) \quad (9)$$

- From Equation 13 it follows that

$$c_{\text{in}}(t) = c_{\text{eq}} + (c_0 - c_{\text{eq}})e^{-t/\tau_{\text{eff}}}, \quad (10)$$

$$c_{\text{in}}(t) = \phi c_0 + (1-\phi)\left[c_{\text{ex}} + (c_0 - c_{\text{ex}})\, e^{-\frac{t}{\tau(1-\phi)}}\right] \quad (11)$$

- The deviation of any concentration from equilibrium,

$$\delta(t) = c_{\text{in}}(t) - c_{\text{eq}}, \quad (12)$$

relaxes exponentially:

$$\delta(t) = \delta(0)e^{-t/\tau_{\text{eff}}}, \quad (13)$$

$$\delta(0) = c_0 - c_{\text{eq}} \quad (14)$$

ALIGNMENT OF COMPUTATIONAL METHODS

Comparison to spore-scale numerical scheme

- This new analytical formula is the **closest mathematical representation** so far of the saturation phenomena from the numerical simulations.
- The deviation could be coming from
  - a numerical error;
  - the representation of the spore as a cube

  in the numerical simulation.

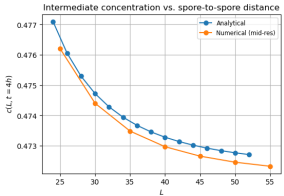

Figure: Centre-to-centre distance vs. concentration at $t = 1$ h.

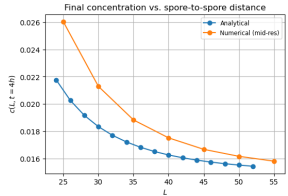

Figure: Centre-to-centre distance vs. concentration at $t = 4$ h.

ALIGNMENT OF COMPUTATIONAL METHODS

Overall model comparison

- It can be concluded that:
  - at low ρ_s, all models align with the analytical **simple permeation** model;
  - the **super-spore scale** model becomes too coarse at high ρ_s, cannot represent saturation well;
  - the **cell-wall scale** model may suffer from rounding errors due to its fine granularity;
  - the **spore-scale** numerical model and the **volume-based analytical model** exhibit the best alignment, despite coming from different formulations.

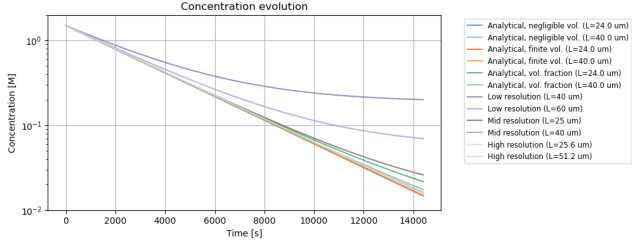

OUTLINE

1 Alignment of computational methods
- Overview
- Volume-based saturation formula
- Overall model comparison

2 Single-spore experiments: revision
- Introduction
- Glucose as a reference molecule
- Diffusion and permeation constants
- Inhibitor concentrations
- Single-spore release scenarios

3 Spore cluster experiments: revision
- Introduction
- Homogeneous vs. cell-wall-bound inhibitor
- Extreme cases
- Functional relationship

4 Next steps

SINGLE-SPORE EXPERIMENTS: REVISION

- The goal is to test if **interface permeability theory** (spore as a "leaky balloon") can be used to estimate meaningful properties of a non-replenishable germination inhibitor released by the spore.
- The release from a single spore is simulated in isolation using numerical and analytical methods.

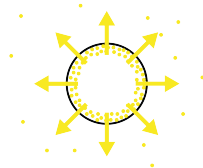

SINGLE-SPORE EXPERIMENTS: REVISION

Glucose as a reference molecule

- Glucose has a size very similar to 1-octen-3-ol and has been widely studied.
- Known diffusivities:
  - the diffusion constant of glucose in water is $D = 6 \times 10^{-6}\ \mathrm{cm}^2/\mathrm{s} = 600\ \mu\mathrm{m}^2/\mathrm{s}$ [4];
  - the diffusion constant of glucose in an agarose film is $D = 6.38 \times 10^{-6}\ \mathrm{cm}^2/\mathrm{s} = 638\ \mu\mathrm{m}^2/\mathrm{s}$ [9];
  - the diffusion constant of glucose in cellulose nanofibrils is $D = 1.7 \times 10^{-7}\ \mathrm{cm}^2/\mathrm{s} = 17\ \mu\mathrm{m}^2/\mathrm{s}$ [3].

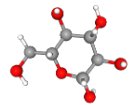

Figure: Glucose

SINGLE-SPORE EXPERIMENTS: REVISION

Diffusion constants

- The diffusion constant of 1-Octen-3-ol in water can be obtained from the Stokes-Einstein relation

$$D = \frac{k_B T}{6\pi\eta a}, \tag{15}$$

considering a temperature of $T = 303.15$ K, a thermodynamic constant of $k_B T = 4.18 \times 10^{-21}$ J and a water viscosity $\eta = 0.797$ mPa s.

Figure: 1-octen-3-ol

- The Stokes radius computed from its molecular volume is

$$a(\text{1-octen-3-ol}) = \left(\frac{3}{4\pi} V_M\right)^{1/3} = 0.393 \text{ nm}. \tag{16}$$

- Therefore,

$$D(\text{1-octen-3-ol in water}) \approx 6.9016 \times 10^{-6} \text{ cm}^2/\text{s} = 690.16\, \mu\text{m}^2/\text{s}. \tag{17}$$

SINGLE-SPORE EXPERIMENTS: REVISION

Diffusion constants

- Alternatively, one can use the ratio of the Stokes radii of 1-octen-3-ol (0.393 nm) and glucose (0.36 nm) to scale the *empirically measured* diffusivity of glucose to that of 1-octen-3-ol:

$$D(\text{1-octen-3-ol in water}) = \frac{a(\text{glucose})}{a(\text{1-octen-3-ol})} \times D(\text{glucose in water})$$
$$\approx 6.55 \times 10^{-6}\ \text{cm}^2/\text{s} = 655\ \mu\text{m}^2/\text{s}. \quad (18)$$

Figure: 1-octen-3-ol

- This is slightly lower than the other estimate, but it has to be noted that the viscosity is somewhat sensitive to the temperature assumption.

SINGLE-SPORE EXPERIMENTS: REVISION

Diffusion constants

- This means other diffusion constants can be estimated like this as well!
  - $D(\text{1-octen-3-ol in agarose}) \approx D(\text{1-octen-3-ol in water})$,
  - $D(\text{1-octen-3-ol in cellulose}) \approx \frac{a(\text{glucose})}{a(\text{1-octen-3-ol})} \times D(\text{glucose in cellulose}) = 1.56 \times 10^{-7}\ \text{cm}^2/\text{s} = 15.6\ \mu\text{m}^2/\text{s}$.
- Other volatile organic compounds (VOCs) like **3-octanone** and **3-octanol** have a very similar Stokes radius and can be considered to have the same diffusivities.
- A potential heat-labile peptide ($a = 6$ nm as to permeate the cell wall [2]) has
  - $D(\text{heat-labile peptide in water}) \approx 4.54855 \times 10^{-7}\ \text{cm}^2/\text{s} = 45.4855\ \mu\text{m}^2/\text{s}$,
  - $D(\text{heat-labile peptide in cellulose}) \approx \frac{a(\text{glucose})}{a(\text{heat-labile peptide})} \times D(\text{glucose in cellulose}) = 1.02 \times 10^{-8}\ \text{cm}^2/\text{s} = 1.02\ \mu\text{m}^2/\text{s}$.

Figure: 3-octanone

Figure: 3-octanol

SINGLE-SPORE EXPERIMENTS: REVISION

Permeation constants

- The permeation constant of glucose in synthetic lipid bylayer found in literature is $P_s = 1.4 \times 10^{-10}$ cm/s [1] or $P_s = 2.4 \times 10^{-10}$ cm/s [5]. A rough average of $P_s = 2.0 \times 10^{-10}$ cm/s is taken.
- In **lipid membranes**, the permeation constant is linked to the diffusion constant via the **Meyer-Overton** rule:

$$P_s = \frac{KD}{d}, \tag{19}$$

  where $d = 3.8$ nm in liquid-phase lipid bilayers [8].
- Then,
  - $P_s(\text{1-octen-3-ol through lipid bilayer}) = \frac{K(\text{1-octen-3-ol}) \cdot D(\text{glucose in lipid bilayer})}{d} \times \frac{a(\text{glucose})}{a(\text{1-octen-3-ol})} \approx 9.04 \times 10^{-5}$ cm/s $= 0.904$ μm/s.

SINGLE-SPORE EXPERIMENTS: REVISION

Permeation constants

- In porous barriers, filled with water, that weakly interact with the solute, the partition coefficient can be approximated to $K \approx 1$, indicating a lack of preference for the molecule to reside inside or outside the barrier.
- Other factors like the porosity of the barrier can be absorbed in an effective permeation constant $P_{\text{eff}} \approx \frac{D}{d}$.
- Considering a 400 nm thick barrier (upper estimate [7]), we can compute
  - $P_{\text{eff}}(\text{1-octen-3-ol through agarose}) = \frac{D(\text{1-octen-3-ol in agarose})}{d} \approx \frac{D(\text{1-octen-3-ol in water})}{d} = \frac{690\ \mu\text{m}^2/\text{s}}{0.4\ \mu\text{m}} = 0.1725\ \text{cm/s} = 1725\ \mu\text{m/s}$,
  - $P_{\text{eff}}(\text{1-octen-3-ol through cellulose}) = \frac{D(\text{1-octen-3-ol in cellulose})}{d} = \frac{15.6\ \mu\text{m}^2/\text{s}}{0.4\ \mu\text{m}} = 0.0039\ \text{cm/s} = 39\ \mu\text{m/s}$.

SINGLE-SPORE EXPERIMENTS: REVISION

Permeation constants

- Proteins usually permeate cell membranes via channels or transporters, so a cell-membrane permeability is hard to define.
- In polysaccharides,
  - $P_{\text{eff}}(\text{heat-labile peptide through agarose}) = \frac{D(\text{heat-labile peptide in agarose})}{d} \approx \frac{D(\text{heat-labile peptide in water})}{d} = \frac{45.4855}{0.4\ \mu\text{m}} = 0.011371375\ \text{cm/s} = 113.71375\ \mu\text{m/s}$,
  - $P_{\text{eff}}(\text{heat-labile peptide through cellulose}) = \frac{D(\text{heat-labile peptide in cellulose})}{d} = \frac{1.02\ \mu\text{m}^2/\text{s}}{0.4\ \mu\text{m}} = 2.55 \times 10^{-4}\ \text{cm/s} = 2.55\ \mu\text{m/s}$.

SINGLE-SPORE EXPERIMENTS: REVISION

Summary of diffusivities

	1-octen-3-ol	**heat-labile peptide**
water	$D = 6.9016 \times 10^{-6}\ \mathrm{cm}^2/\mathrm{s}$	$D = 4.54855 \times 10^{-7}\ \mathrm{cm}^2/\mathrm{s}$
lipid bilayer membrane	$P_s = 2.0 \times 10^{-10}\ \mathrm{cm/s}$	N/A
agarose-like cell wall (400 nm)	$P_{\mathrm{eff}} = 0.1725\ \mathrm{cm/s}$	$P_{\mathrm{eff}} = 0.011371375\ \mathrm{cm/s}$
cellulose-like cell wall (400 nm)	$P_{\mathrm{eff}} = 0.0039\ \mathrm{cm/s}$	$P_{\mathrm{eff}} = 2.55 \times 10^{-4}\ \mathrm{cm/s}$

Table: Diffusion coefficients and permeabilities for different substances

» **Assumption:** there is a layer in the cell wall, with the respective properties, that is diffusion limiting (determines the permeation rate of the entire barrier).

SINGLE-SPORE EXPERIMENTS: REVISION

Inhibitor concentrations

- It is important to narrow down
  - what is the **initial inhibitor concentration** in the spore,
  - what is the **concentration threshold** that allows for germination.
- Studies have shown that, after rupturing the cell wall with a freeze-dry cycle, 10^9 *A. flavus* conidia in a 300 μL suspension release not more than 1 μM 1-octen-3-ol [6]. That equals $c_0 \approx 1.5 \times 10^{-5}$ M per conidium.
- A protein in moderate abundance is usually found in the micromolar order ($c_0 \approx 10^{-6}$ M)
- It can be assumed that the inhibitor stops being effective when there are about a hundred molecules left in the spore, at the least. That equals $c_T \approx 2.54 \times 10^{-9}$ M.

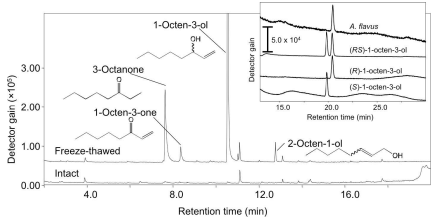

Figure: SPME-GC/MS analysis of volatiles formed from A. flavus conidia [6].

SINGLE-SPORE EXPERIMENTS: REVISION

Intermezzo: inferring c_0 from experimental data

- Studies with *A. nidulans* have documented the effect of **spore crowding** and **added 1-octen-3-ol** on germination.
- Assuming that the analytical model is representative, one can equate the two effects on the concentration at the measured time ($t = 10$ h):

$$\phi c_0 + (1-\phi)\left(c_0 e^{-\frac{t}{\tau(1-\phi)}}\right) = \phi' c_0 + (1-\phi')\left[c_{\text{ex}} + (c_0 - c_{\text{ex}})\, e^{-\frac{t}{\tau(1-\phi')}}\right], \tag{20}$$

  - where c_{ex} are the added concentrations,
  - ϕ are the volume fractions under varying spore densities,
  - ϕ' is the volume fraction when the inhibitor was exogenously added.
- Solving for c_0 in all ϕ and c_{ex} combinations, we get an average $\langle c_0 \rangle \approx 2.58 \times 10^{-9}$ M (quite low but physically sensible).

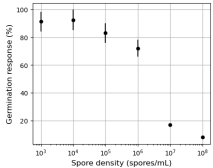

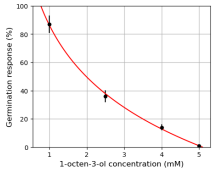

SINGLE-SPORE EXPERIMENTS: REVISION

Single-spore release scenarios

- Testing
  - $c_0 = 1.5 \times 10^{-5}$ M for 1-octen-3-ol and $c_0 = 10^{-6}$ M for a heat-labile peptide,
  - candidate permeabilities / diffusivities and a range of valid germination thresholds,
- it becomes evident that the appropriate permeability lies between cellulose and a lipid bilayer.

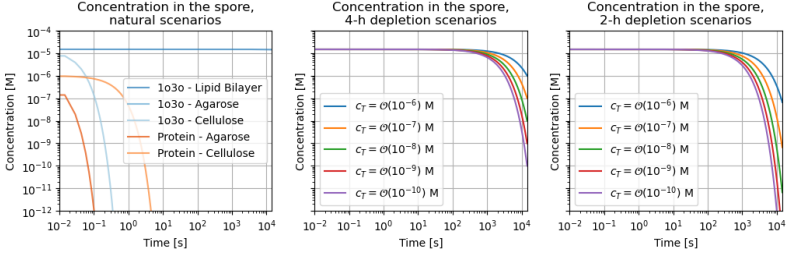

OUTLINE

1 Alignment of computational methods
- Overview
- Volume-based saturation formula
- Overall model comparison

2 Single-spore experiments: revision
- Introduction
- Glucose as a reference molecule
- Diffusion and permeation constants
- Inhibitor concentrations
- Single-spore release scenarios

3 Spore cluster experiments: revision
- Introduction
- Homogeneous vs. cell-wall-bound inhibitor
- Extreme cases
- Functional relationship

4 Next steps

SPORE CLUSTER EXPERIMENTS: REVISION

- Previously, it was found that neighbour clusters affect diffusivity, but this effect could not be reproduced across all models.
- An error was found in the high-resolution solver and was corrected.
- Hence, the cluster simulations were repeated.

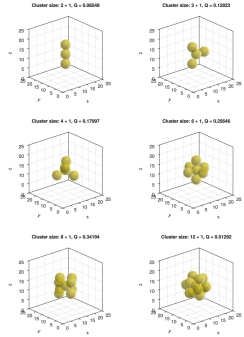

SPORE CLUSTER EXPERIMENTS: REVISION

Homogeneous vs. cell-wall-bound inhibitor

- It was found that, if the inhibitor is **only in the cell wall**, it is released faster compared to a **homogenous distribution** in the spore volume.
- The reason for this is that there is a higher concentration "pressure" for the same amount of molecules.

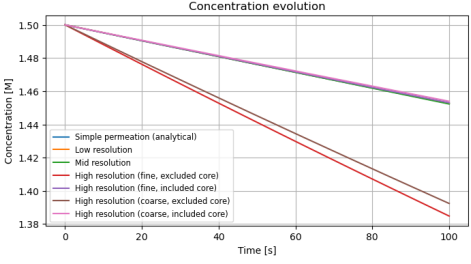

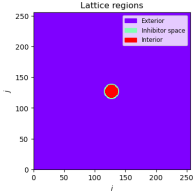

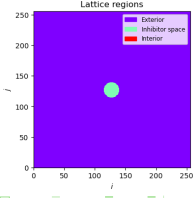

SPORE CLUSTER EXPERIMENTS: REVISION

Extreme cases

- The inhibitor release was compared between a **single spore** and a **full cluster of 12+1 spores**.
- The results show that the neighbours *in direct contact* still obstruct inhibitor release, but to a much lesser degree (7% more residual concentration at $t = 4$ h).
- If the inhibitor is only in the cell wall and the spore interiors are inaccessible, the blocking effect is stronger (20% more residual concentration at $t = 4$ h).

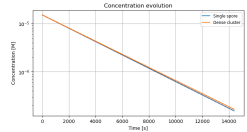

Figure: Empty spore interior.

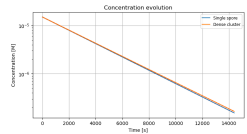

Figure: Full spore interior.

SPORE CLUSTERS VS. RELEASE EXPONENT

Functional relationship

- The neighbour arrangements produce fluctuating results in the measured release exponent.
- The results are sensitive to the arrangement of neighbours around the central spore (symmetric vs. asymmetric).
- Finite lattice size with absorbing boundary possibly distorts the results.
- A fitted power-law yields a relationship $c(t) \sim e^{\alpha t/\tau}$, where $\alpha \sim M^{-0.004}$, i.e. a very slow decrease with increasing number of neighbours M.
- In general, ast diffusion through the cluster gaps still depletes the inhibitor locally. Thus, **clustering is not critical in slowing down inhibitor release**.
- It is to be investigated whether the cluster effect is amplified by the combination of density-driven inhibitor saturation.

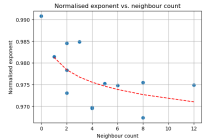

Figure: Empty spore interior.

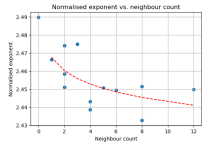

Figure: Full spore interior.

OUTLINE

1 Alignment of computational methods
- Overview
- Volume-based saturation formula
- Overall model comparison

2 Single-spore experiments: revision
- Introduction
- Glucose as a reference molecule
- Diffusion and permeation constants
- Inhibitor concentrations
- Single-spore release scenarios

3 Spore cluster experiments: revision
- Introduction
- Homogeneous vs. cell-wall-bound inhibitor
- Extreme cases
- Functional relationship

4 Next steps

NEXT STEPS

- Turn the **deterministic** model

$$c_{\text{in}}(t) = \phi c_0 + (1-\phi)\left[c_{\text{ex}} + (c_0 - c_{\text{ex}})\, e^{-\frac{t}{\tau(1-\phi)}}\right] \tag{21}$$

  into a **statistical** one to explain experimental data from homogeneous spore cultures.
  - Make assumptions about the distributions of τ, c_0, c_T;
  - Express the probability $P(c(t_{\max}) > c_T | \rho_s)$;
  - Observe how the probability changes with varying ρ_s;
  - Fit to data.
- If the fit is not good, discuss alternative mechanisms:
  - Cell wall adsorption of inhibitor;
  - Inhibitor interactions.

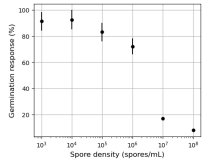

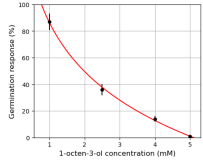

BIBLIOGRAPHY I

[1] G J Bresseleers, H. L. Goderis, and Paul P. Tobback. “Measurement of the glucose permeation rate across phospholipid bilayers using small unilamellar vesicles. Effect of membrane composition and temperature.”. In: *Biochimica et biophysica acta* 772 3 (1984), pp. 374–82. URL: https://api.semanticscholar.org/CorpusID:9584953.

[2] Stanley Brul, J Nussbaum, and S. K. Dielbandhoesing. “Fluorescent probes for wall porosity and membrane integrity in filamentous fungi”. In: *Journal of Microbiological Methods* 28 (1997), pp. 169–178. URL: https://api.semanticscholar.org/CorpusID:85293622.

[3] Nicklaus Carter, Julia Towne, and David J. Neivandt. “Finite element analysis of glucose diffusivity in cellulose nanofibril peripheral nerve conduits”. In: *Cellulose* 28 (2021), pp. 2791 –2803. URL: https://api.semanticscholar.org/CorpusID:231858923.

[4] Rudolf Hober. “Physical chemistry of cells and tissues”. In: 1945. URL: https://api.semanticscholar.org/CorpusID:11597902.

BIBLIOGRAPHY II

[5] Henry V Jakubowski et al. “Fundamentals of Biochemistry, a free and new LibreText book for Undergraduate Courses”. In: *The FASEB Journal* 36 (2022). URL: https://api.semanticscholar.org/CorpusID:248635799.

[6] Kana Miyamoto et al. “Formation of 1-octen-3-ol from Aspergillus flavus conidia is accelerated after disruption of cells independently of Ppo oxygenases, and is not a main cause of inhibition of germination”. In: *PeerJ* 2 (2014). URL: https://api.semanticscholar.org/CorpusID:8514039.

[7] Benjamin D. Strycker et al. “CARS spectroscopy of Aspergillus nidulans spores”. In: *Scientific Reports* 9 (2019). URL: https://api.semanticscholar.org/CorpusID:59945452.

[8] Fiona Yarrow and Bonny W M Kuipers. “AFM study of the thermotropic behaviour of supported DPPC bilayers with and without the model peptide WALP23.”. In: *Chemistry and physics of lipids* 164 1 (2011), pp. 9–15. URL: https://api.semanticscholar.org/CorpusID:25188407.

BIBLIOGRAPHY III

[9] Tong Zhang and Hff Fang. “Effective Diffusion Coefficients of Glucose in Artificial Biofilms”. In: *Environmental Technology* 26 (2005), pp. 155 –160. URL: https://api.semanticscholar.org/CorpusID:41242504.